City, University of London Institutional Repository

A Numerical study for Chloride Migration in Concrete Under Electrochemical Repair Process

Xuandong Chen[1,2,3], Qing Zhang[1], Yang Ming[3], Feng Fu[4*], and Hua Rong[5]

[1] College of Mechanics and Materials, Hohai University, Nanjing, 211100, People's Republic of China

[2] College of Civil and Architecture Engineering, Guilin University of Technology, Guilin 541004, People's Republic of China.

[3] Guangxi Key Laboratory of New Energy and Building Energy Saving, Guilin 541004, People's Republic of China.

[4] School of Mathematics, Computer Science and Engineering, City, University of London, London EC1C,0HB U.K.

[5] Central Research Institute of Building and Construction, Beijing 100088, People's Republic of China

* Corresponding author: E-mail address: feng.fu.1@city.ac.uk

Abstract: Electrochemical repair is one of the most effective methods of removing chloride from offshore engineering structures to improve their durability. The diffusion of chloride and electrochemical repair are key stages in this process. In this paper, a new numerical chloride migration-diffusion model is established by using Nernst-Planck equation. The distributions of free chloride ions in concrete in the stage of free chloride diffusion and the stage of electrochemical repair are simulated, and the effects of external potential and cathode position on electrochemical repair efficiency are analyzed. The numerical results show that electrochemical repair can effectively remove chloride ions from concrete. After 12 weeks of the electrochemical repair, the electrochemical repair efficiency is more than 66%. With the increase of repair time, the increase amplitude of electrochemical repair efficiency decreases gradually. In the initial stage of electrochemical repair, the chloride concentration on reinforcing bar surface decreases rapidly. After 4 weeks of electrochemical repair, the chloride concentration tends to be stable. As external potential increases, the electrochemical repair efficiency is also improved, and the chloride concentration on reinforcing bar surface decreases rapidly. When the cathodes are set on both sides of the concrete, the electrochemical repair time should be extended, and external potential should be increased to achieve better repair effect.

Key words: Electrochemical repair; Numerical simulation; Chloride Migration; Concrete Durability

1 Introduction

In offshore engineering structures, chloride is one of the main factors causing reinforcing bar corrosion (Arya, Vassie and Bioubakhsh, 2014; Kumar, Kumar and Kujur, 2019; Wang, Gong and Wu, 2019). Electrochemical repair is one of effective methods to remove chloride in concrete and improve the durability of offshore engineering structures (Xia *et al.*, 2019). Electrochemical chloride removal (ECR) technique refers to the formation of potential difference between reinforcing bar (*i.e.*, cathode) and external electrolyte (*i.e.*, anode). Under the action of potential difference, chloride in concrete moves from low potential to high potential, so as to remove chloride in concrete (Shi *et al.*, 2012; Xia *et al.*, 2019; Xu and Li, 2019a).

ECR technique has been favored by many research scholars since the experimental investigation work was carried out in the 1970s (Garcés, Sánchez De Rojas and Climent, 2006; Miranda *et al.*, 2007; Sánchez and Alonso, 2011). Mao *et al.*(Mao *et al.*, 2015) studied the effect of external electric field on chloride removal in sea sand concrete. And the research indicated that external electric field could effectively remove chloride in sea sand concrete, and the durability of sea sand concrete could be greatly improved by migrating corrosion inhibitor into reinforcing bar surface. The study of Zhou *et al*. (Zhou *et al.*, 2020) manifested that external electric field could effectively remove chloride in concrete, but it also led to the migration and aggregation of a large number of K^+ and Na^+ ions to the arear near the reinforcing bar. Saraswathy *et al*. (Saraswathy, H.-S. Lee, *et al.*, 2018) investigated the effect of different anode types on chloride removal efficiency. Xia, J. *et al*. (Xia, Q. Liu, *et al.*, 2018) discussed the effect of ambient temperature on ECR efficiency. The study displayed that the total efficiency was doubled as the temperature increased from 0°C to 20°C, and it was improved by 13% as the temperature reached 50°C, indicating that temperature rise was an effective method of improving ECR efficiency. However, concrete is a heterogenous material with complex microstructure. Due to the interaction between different factors, it's hard to determine the individual effects of various factors through experiments. Comparatively speaking, numerical models have great advantages in providing detailed information and studying research parameters.

With the progress of computer science and technology and the development of finite element numerical method, especially for complicated multi-field coupling problems, numerical simulation technique has been extensively applied. In the existing ECR numerical models (Li and Page, 1998; Toumi, François and Alvarado, 2007; Xia, Q. feng Liu, *et al.*, 2018), it's assumed that concrete was isotropic material, and Nernst-Planck equation was used to simulate the chloride removal process of reinforced concrete under the action of potential. The effects of treatment time, current density, binding effect, additive, and temperature on ECR efficiency were studied. Li, *et al.* (Li and Page, 2000) established a numerical electrochemical chloride removal model by using Nernst-Planck

71 equation, and solved the Nernst-Planck equation by employed finite element method. And the
72 effects of external current density, treatment time, ion coefficient, ion binding, boundary condition
73 and medium porosity on chloride extraction efficiency were studied. Xu, Jun et al. (Xu and Li,
74 2019b) established the fitting formulas of chloride removal efficiency of unilateral-anode concrete
75 with current density and treatment time. Liu, Q., *et al*. (Liu *et al.*, 2015) discussed the effects of
76 aggregate shape, boundary conditions and double electrode layers on ECR efficiency and ion
77 concentration distribution.

78   Many researchers have conducted a large quantity of fundamental studies on ECR, providing
79 a theoretical and experimental basis for follow-up ECR researches (Liu *et al.*, 2014). However, all
80 of the abovementioned researches are based on uniform chloride distribution in concrete. While in
81 practical engineering, the distribution of chloride in concrete is nonuniform. The concentration of
82 chloride ions near the erosion surface is higher, while the chloride concentration away from erosion
83 surface is lower. In this paper, the distribution of free chloride in practical engineering is simulated
84 through two stages, *i.e.*, the diffusion of free chloride and electric migration. The external electric
85 field is applied to remove chloride ions diffused into the concrete. The numerical electrochemical
86 repair model with diffusion-electric migration is established, and the chloride distribution laws in
87 the concrete are investigated.

2. Theoretical background

2.1 Chloride diffusion

90   In offshore engineering structures, chloride ions in the environment diffuse into the concrete
91 due to the chloride concentration difference (Chen *et al.*, 2020, 2021). The studies of many
92 researchers indicates that chloride diffusion conforms to Fick's second Law, and the chloride
93 diffusion equation in the concrete is as follow (DHIR, JONES and MCCARTHY, 1993; Jin *et al.*,
94 2015; Zhu and Zi, 2017; Mazer, Lima and Medeiros-Junior, 2018; Wang *et al.*, 2018):

$$\frac{\partial C}{\partial t} = \nabla \left(D_{cl} \nabla C \right) \tag{1}$$

96 where *t* is the erosion time of chloride, C is the chloride concentration (by weight of concrete, %),
97 and D_{cl} is chloride diffusion coefficient, respectively. It can be seen from Eq. (1) that D_{cl} is a
98 decisive factor for chloride concentration in concrete. The chloride ion diffusion coefficient not only
99 relates to the concrete itself (such as concrete type, pore structure, water-binder ratio, hydration
100 degree and so on), but also relates to the external environment, such as temperature (Bažant and
101 Najjar, 1972), humidity (Muthulingam and Rao, 2014), maintenance age (Martín-Pérez,
102 Pantazopoulou and Thomas, 2001) and other factors. In this paper, only the effects of water-binder
103 ratio, temperature, humidity, and age are considered in the chloride diffusion coefficient. And the

chloride diffusion coefficient can be expressed as (Jin *et al.*, 2015; Wang *et al.*, 2018; Chen *et al.*, 2020):

$$D_c = \underbrace{\frac{2 \times \varphi_p^{2.75} D_p}{\varphi_p^{1.75}\left(3-\varphi_p\right)+n\left(1-\varphi_p\right)^{2.75}}}_{\text{Water-cement ratio}} \cdot \underbrace{\exp\left[\frac{U_c}{R}\left(\frac{1}{T_{ref}}-\frac{1}{T}\right)\right]}_{\text{Temperature}} \cdot \underbrace{\left[1+\frac{\left(1-h\right)^4}{\left(1-h_c\right)}\right]^{-1}}_{\text{Humidity}} \cdot \underbrace{\left(\frac{t_{ref}}{t}\right)^m}_{\text{Curing age}} \tag{2}$$

where U_c is the chloride diffusion activation energy ($44.6 KJ/mol$), t_{ref} is the reference exposure time (28 d), t is the chloride ion erosion time (s), T is the ambient temperature (K), R is the gas constant ($8.314 J/K \cdot mol$), T_{ref} is the reference temperature ($298 K$), h is the humidity and h_c the critical humidity (0.75). D_p is the chloride diffusion coefficient in water (1.07×10^{-10} m^2/s), n is the empirical parameter (14.44) (Du, Jin and Ma, 2014), m is the time attenuation index. And φ_p is the porosity of cement paste, which can be expressed as (Sun *et al.*, 2011)

$$\varphi_p = \frac{wc - 0.17\alpha}{wc + 0.32} \tag{3}$$

where α is the degree of hydration of cement paste, and wc is the ratio of water to binder.

2.2 Electrochemical migration

As is known, the concrete pore solution contains various ions. Under the action of external electric field, positively charged ions move towards low potential, and negatively charged ones move towards high potential (Liu *et al.*, 2015; Chen *et al.*, 2021). Assuming that the concrete pore solution is diluted solution and the internal ions do not react with each other, the ion concentration in the concrete under the action of electric field can be calculated according to Nernst-Planck equation. The material equilibrium and ion transfer are defined by combing electric neutrality condition (Xu and Li, 2019a; Chen *et al.*, 2021; Fang *et al.*, 2021).

$$\frac{\partial C_i}{\partial t} = \nabla\left(D_i \nabla C_i + z_i D_i\left(\frac{F}{RT}\nabla\phi\right)C_i\right) \tag{4}$$

$$I = F\sum_{i=1}^{n} z_i\left(-D_i \nabla C_i - z_i D_i\left(\frac{F}{RT}\nabla\phi\right)C_i\right) \tag{5}$$

$$\sum_{i=1}^{n} z_i C_i = 0 \tag{6}$$

where C_i, D_i, and z_i represent the concentration, diffusion coefficient and charge number of the *i*-th ionic species in concrete, respectively. $F = 9.648 \times 10^4 C \cdot mol^{-1}$ is the Faraday constant, ϕ is the electric potential.

3 Numerical simulations

During concrete pouring process in the actual projects, the concrete pore solution contains various ions, mainly including K^+, Na^+, Ca^{2+} and OH^- ions. These ions are formed during the pouring

132 process and are uniform distribution in the concrete. The chloride content is very small and can be

133 ignored during the pouring process. However, during the service process of concrete, chloride ions

134 in the environment gradually penetrated concrete. The free chloride diffusion process is simulated

135 by Eq. (1), in which the external electric field is not applied. After chloride diffusion for a certain

136 time, an external electric field is applied to remove chloride ions from concrete. The ion

137 concentration distributions at different time are calculated by Eqs. (4) ~ (6).

138   Wu *et al*. (Wu, Li and Yu, 2017) performed on-situ chloride sampling and testing at 13# wharf

139 of Fangcheng Port, Beibu Gulf in Guangxi Province. The results showed that the chloride

140 concentration in the outmost layer was about 0.67%, which was converted into Molar concentration

141 of 471.8 mol/m^3. Therefore, the boundary concentration of chloride ions on the erosion surface is

142 taken as 471.8 mol/m^3 in this paper. In the 10th year after chloride ion free erosion, electrochemical

143 repair is started. The chloride concentration in the concrete is CL_{10}, and the chloride diffusion

144 coefficient is D_{cl10}. The boundary concentrations and diffusion coefficients of other ions can refer

145 to references shown in **Tab. 1**. **Fig. 1** is the schematic diagram of chloride attack on concrete and

146 electrochemical repair. The diameter of the reinforcing bar is 12 mm, the thickness of the concrete

147 cover is 60 mm, and the geometric dimension of concrete section is 150 mm x 150 mm, respectively.

148

(a) Seawater erosion   (b) Electrochemical repair 1   (c) Electrochemical repair 2
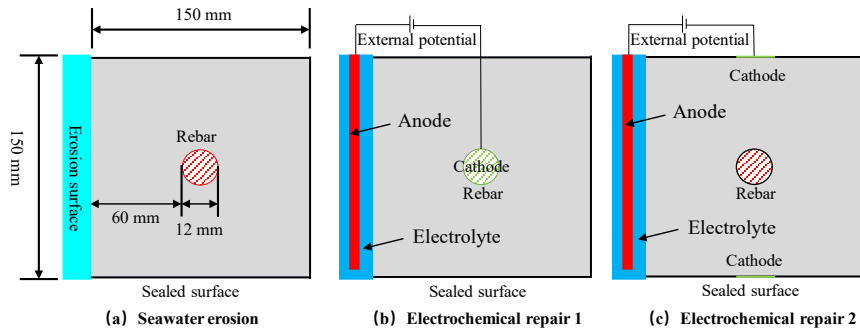
149 **Fig. 1.** Numerical simulation diagram.

150 **Table 1** Boundary conditions, initial values, and diffusion coefficients of various ion (Wang, Li and Page, 2001;

151 Liu *et al.*, 2012; Xia *et al.*, 2020).

Field variables	Position	K^+	Na^+	Ca^{2+}	OH^-	Cl^-
Charge number	--	+1	+1	+2	-1	-1
Boundary concentration (mol/m^3)	Anode	5	5	25.2	12.6	10
Flux boundary condition	Sealing	0	0	0	0	0
Initial concentration (mol/m^3)	Internal	100	Cl_{10}	Cl_{10}	100	0

| Diffusion coefficient (m²/s) | -- | 3.9×10^{-11} | 2.7×10^{-11} | 1.6×10^{-11} | 5.28×10^{-10} | D_{cl} |

4. Result analysis and discussion

4.1 Chloride concentration distribution

(a) Before repair   (b) Repair 1 week   (c) Repair 4 weeks

(d) Repair 8 weeks   (e) Repair 12 weeks
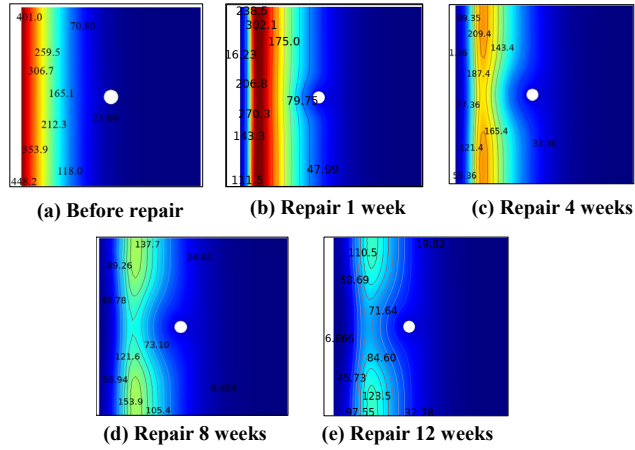
Fig. 2. Chloride concentration distribution cloud map.

Fig. 2a shows the free chloride concentration distribution in the 10th year of chloride diffusion. In the electrochemical repair process, the reinforcement bar is used as cathode, as shown in **Fig. 1b**. And the applied electric potential is 12 V. Additionally, the distributions of free chloride with different electrochemical repair time are shown in **Fig. 2b-e.** It can be seen from **Fig. 2a-e** that under the action of external electric field, chloride ions are removed from concrete. The chloride distributions in the concrete after electrochemical repair (as shown in **Fig. 2b-e**) are very different from that in the free diffusion stage (as shown in **Fig. 2a**). Compared with that before electrochemical repair (as shown in **Fig. 2a**), the chloride concentrations near the erosion surface (as shown in **Fig. 2b-e**)are lower after electrochemical repair. With the increase of erosion depth, chloride concentration first gradually increases and then decreases. Chloride ions migrate outward rapidly due to the applied low electric field around the reinforcing bar. With the increase of electrochemical repair time, the total chloride content in concrete gradually decreases, indicating that electrochemical repair is an effective method to remove chloride ions from concrete.
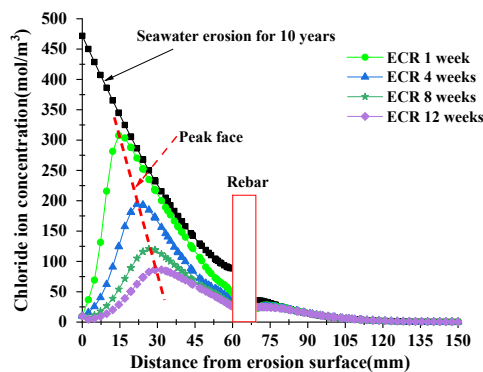
170 **Fig. 3.** Chloride concentration along the depth distribution curve

171   **Fig. 3** shows the chloride concentration distribution curves in concrete at 1week, 4 weeks, 8

172 weeks, and 12 weeks of electrochemical repair. It is obvious from **Fig. 3** that the peak value of

173 chloride concentration in concrete appear at 15 mm~30 mm away from the erosion surface. With

174 the increase of the electrochemical repair time, the peak concentration of chloride gradually

175 decreases and gradually moves towards the interior of concrete, which indicates that chloride ions

176 in concrete are continuously remove from concrete under the action of external electric field. After

177 12 weeks of electrochemical repair, the peak value of chloride concentration decreases to 86.55

178 mol/m^3. Additionally, the chloride concentration near the erosion surface changes obviously, while

179 the change of chloride concentration on the other side of erosion surface is not obvious. Similar

180 conclusions were also found in the study of Chen *et al* (Chen *et al.*, 2021).

181 **4.2 Chloride concentration on reinforcing bar surface**

182   For reinforced concrete, the chloride concentration on the reinforcing bar surface is one of

183 critical factors influencing corrosion of reinforcing bar. The chloride concentration on the

184 reinforcing bar surface under the action of external electric field will be analyzed in this section. It

185 should be noted that the position and applied potential of the cathode are the same as those in Section

186 4.1. *i.e.,* the reinforcing bar is used as cathode and the applied electric potential is 12 V. **Fig. 4** shows

187 the chloride concentration curves at three different points on the reinforcing bar surface. It is

188 apparent from **Fig. 4** that the chloride concentrations at three positions decrease with the increase

189 of electrochemical repair time. Moreover, in the first 14 days (14 d) of electrochemical repair, the

190 chloride concentrations decrease sharply and then tended to be stable (about 24 mol/m^3). This

191 indicates that the electrochemical repair efficiency cannot be improved by prolonging the repair

192 time when the electrochemical repaired has been carried out for a certain time.

193
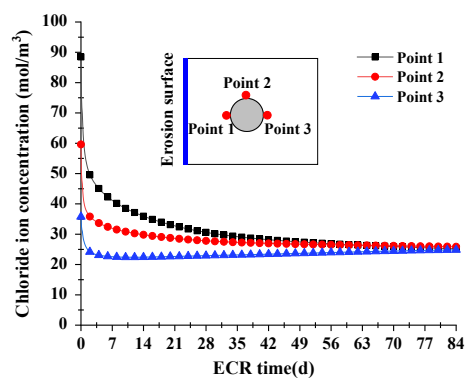
194   **Fig. 4.** Chloride concentration curves on the reinforcing bar surface.

195 **4.3 ECR efficiency**

196   Chloride diffusion is a very slow process, the total chloride content in the concrete has a great

197 influence on the redistribution of chloride after the ECR. Therefore, the total chloride reduction rate

198 in concrete is employed in this paper as an evaluation index measuring the repair effect. The

199 calculation formula is as below:

$$P = \frac{M_0 - M_t}{M_0} \times 100\% \qquad (7)$$

201 where P is the chloride ion reduction rate (%), M_0 is the total amount of initial chloride ion in

202 concrete (mol), M_t is the total concentration of chloride ion in concrete at the time of

203 electrochemical repair (mol).

204   The reinforcing bar is used as cathode and the applied electric potential is 12 V **Fig. 5** shows

205 the histogram of chloride removal rate in concrete at different repair time. It is obvious from **Fig. 5.**

206 that at 1 week, 4 weeks, 8 weeks and 12 weeks of the electrochemical repair, the chloride removal

207 rates are 24%, 45%, 58% and 66%, respectively. This indicates that the electrochemical repair could

208 effectively remove chloride ions in concrete. Meanwhile, with the increase of repair time, the

209 increase amplitude of chloride removal rate gradually decreases. Similar phenomenon has also been

210 found by Saraswathy *et al*. (Saraswathy *et al*. 2017) and Chen et al. (*Chen et al.,* 2021).
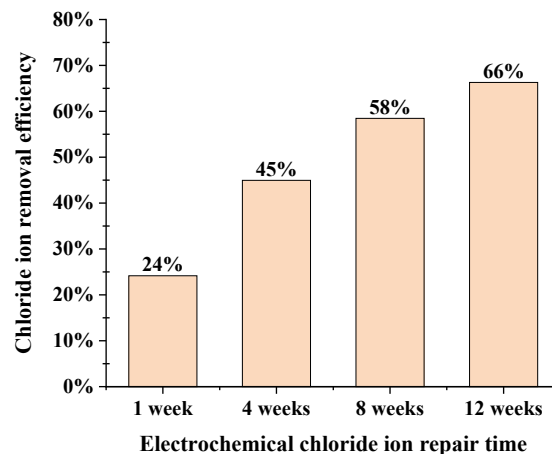

211

212   **Fig. 5.** ECR efficiency at different repair times.

213 **4.4 Effect of different potentials on ECR**

214   According to formula (4), the potential gradient is the main driving force for chloride migration.

215 Therefore, the potential difference between anode and cathode plays a very important role in

216 chloride removal rate. **Fig. 6a-c** shows the distributions of chloride concentration at 12 weeks of the

217 electrochemical repair under potentials of 5 V, 12 V and 24 V, respectively. It can be seen from **Fig.**

218 **6a-c** that the chloride concentration in concrete gradually decreases with the increase of potential.

219 For different potentials, the overall chloride concentration are different, while the chloride

220 distribution trend in concrete doesn't changed significantly. It is obvious from that **Fig. 6a-c** two

221 chloride concentration peak points are formed on the side near the erosion surface. Through

comparing **Fig. 6a**, **b** and **c**, it is apparent that the chloride concentration difference between **Fig. 6a** and **b** is very large, while the chloride concentration difference between **Fig. 6b** and **c** is relatively small. This indicates that as the potential increase, the influence of potential on chloride concentration distribution decreases.

(a) Potential=5V   **(b) Potential=12V**   **(c) Potential=24V**
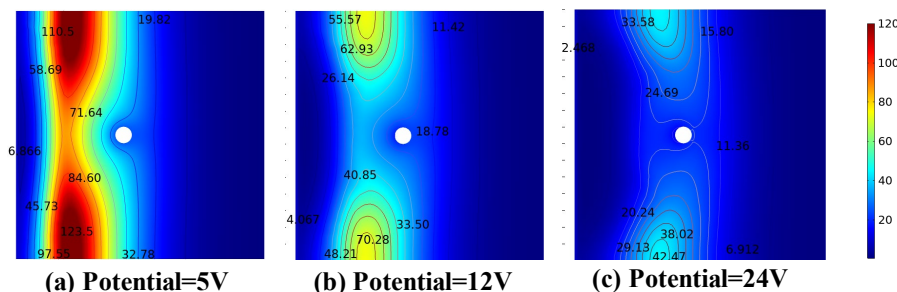
Fig. 6. Cloud images of different potential potentials.

**Fig. 7** shows the chloride removal rate histograms at 1 week, 4 weeks, 8 weeks, and 12 weeks of electrochemical repair under different potentials. It can be seen from **Fig. 7** that increasing potential can effectively improve the chloride removal rate. However, too high potential may cause hydrogen evolution reaction on the reinforcing bar surface and make the reinforcing bar more fragile (Mao *et al.*, 2019; Chen *et al.*, 2021). At 12 weeks of the electrochemical repair, the chloride removal rates under external potentials of 5 V, 12 V and 24 V are 66%, 81% and 88%, respectively., respectively. Compared with the electrochemical repair time of 8 weeks, the chloride removal rates under external potentials of 5 V, 12 V and 24 V at the electrochemical repair time of 12 weeks increase by 8%, 6% and 3%, respectively. While compared with the electrochemical repair time of 4 weeks, the chloride removal rates under external potentials of 5 V, 12 V and 24 V at the electrochemical repair time of 8 weeks increase by 3%, 13% and 10%, respectively. These results indicate that the increase of ECR efficiency decreases gradually with the increase of electrochemical repair time. The chloride migration is mainly driven by electric migration in the early stage of electrochemical repair, while it is mainly driven by the concentration difference in later stage of electrochemical repair.
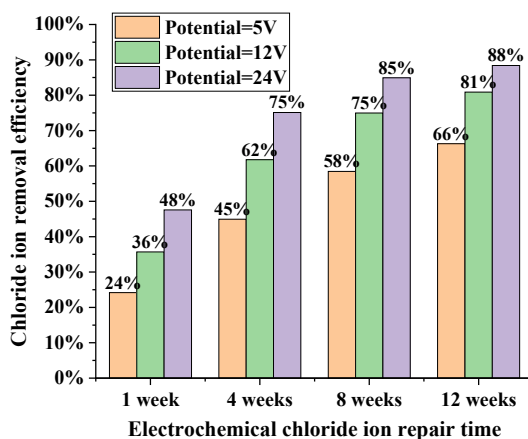
245   **4.5 Effect of cathode location on ECR**

246   According to the above analysis, the electrochemical repair can effectively remove chloride

247   ions in concrete. However, many studies show that ECR will not only eliminate harmful chloride

248   ions, but also have adverse effects on reinforced concrete structure, such as reducing the bonding

249   strength between reinforcing bar and concrete (Nguyen *et al.*, 2021), making the reinforcing bar

250   more fragile (Saraswathy, H. S. Lee, *et al.*, 2018). Meanwhile, Na^+ and K^+ ions in the concrete

251   solution will also aggregate near the reinforcing bar, causing concrete ASR harm. In this section,

252   the chloride distributions in concrete and the ECR efficiency are analyzed when the reinforcing bar

253   is used as cathode and both sides of concrete are used as cathodes. **Fig. 8a-b** show the chloride

254   distributions in concrete at 8 weeks of electrochemical repair. It is apparent from **Fig. 8a-b** that there

255   is great difference in the chloride distributions in concrete with these two cases. Generally, the

256   reinforcing bar is taken as cathode, as is shown in **Fig. 8a**. And the chloride ion concentration near

257   the reinforcement is the lowest, and two peaks of chloride ion concentration are formed in the

258   concrete. When both sides of concrete are used as cathodes, chloride ions move from both sides of

259   the concrete (*i.e.*, cathodes) to the erosion surface (*i.e.*, anode), as is shown in **Fig. 8b**. This results

260   in the lowest chloride concentration on both sides of the concrete (*i.e.*, cathodes) and the highest

261   chloride concentration near the surface of the reinforcement, as is shown in **Fig. 8b**. And a chloride

262   ion concentration peak appears near the reinforcement surface in concrete. Moreover, by comparing

263   **Fig. 8a** and **b**, the peak values of the two cases are almost the same, *i.e.*, about 100 mol/m^3.

(a) Conventional model   (b) Innovative model

264
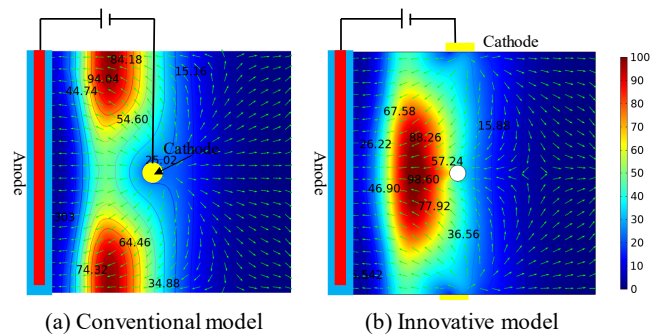
265   **Fig. 8.** Chloride distributions in concrete with different cathode positions at 8 weeks of electrochemical repair. (a)

266   Reinforcing bar is used as cathode, and (b   both sides of concrete are used cathodes.

267

268   **Fig. 9** shows the distributions of chloride ion concentration on the surface of reinforcement

269   with erosion time when reinforcement is used as cathode and both sides of concrete are used as

270   cathode, respectively. It can be seen from **Fig. 9** that under the same external potential of 12 V, the

271   chloride concentration on the reinforcing bar surface in the model with cathodes on both sides of

272   concrete (red dot curve) is much higher than that with cathode on the reinforcing bar (black square

curve). Moreover, in the model with reinforcing bar as cathode, the chloride concentration on the surface of reinforcing bar (black square curve) decreases rapidly and tends to be stable after 14 d of electrochemical repair. However, for the model with both sides of concrete as cathodes, the chloride concentration (red dot curve) decreases slowly with electrochemical repair time. Additionally, the chloride concentration curves with both sides of concrete as cathodes under external potentials of 12 V, 24 V and 36 V are also depicted in **Fig. 9**. It is obvious from **Fig. 9** that the chloride concentration on the reinforcing bar surface can be effectively reduced by increasing the external potential. However, the overall electrochemical repair effect in the model with cathodes on both sides of concrete is still worse than that in the model with reinforcing bar served as cathode. Nevertheless, from the curve declining trend analysis, the model in which the two sides of concrete served as the cathode can achieve better chloride removal effect with the increase of electrochemical repair time.
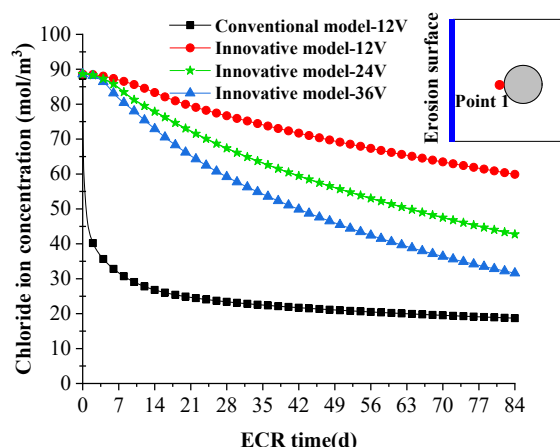
Fig. 9. Chloride ion concentration curves on the surface of steel bars for different repair models.

5 Conclusions

In this paper, a numerical chloride migration-diffusion model is established by Nernst-Planck equation to simulate the chloride erosion process in the external environment and the electrochemical repair process. Based on a systematic study, the following conclusions can be drawn:

(1) Electrochemical repair changes the chloride distribution in concrete. After chloride ions in the external environment diffuse into the concrete, the chloride ions in the concrete can be effectively removed by electrochemical repair. After electrochemical repair, the chloride concentration peak appears at 15 mm ~ 30 mm away from the erosion surface. With the increase of electrochemical repair time, the peak value of chloride concentrate gradually decreases, and the peak of chloride concentrate moves toward the interior of concrete.

(2) Electrochemical repair can rapidly reduce the chloride concentration on the reinforcing bar surface. The chloride concentration on the reinforcing bar surface decreases sharply in the beginning of electrochemical repair and tends to be stable after 14 d of electrochemical repair. Furthermore, with the increase of external potential, the stabilization time is shortened.

301   (3) Electrochemical repair can effectively reduce the chloride concentration in concrete. When
302 the ratio of chloride ion removal in concrete to the total amount of initial chloride ion is used to
303 measure the ECR efficiency, the ECR efficiency can reach more than 60% after 12 weeks of
304 electrochemical repair. Moreover, the ECR efficiency increases with the increase of external
305 potential.

306   (4) When the cathodes are set on both sides of concrete, the ECR efficiency can be improved
307 by increasing the external potential and lengthening the repair time. From a comparison between
308 the situation with cathodes on both sides of concrete and that with cathode on the reinforcing bar
309 surface, it can be found that there is a great difference in chloride concentration after the
310 electrochemical repair. Moreover, the decreasing curves of chloride concentration on the surface of
311 reinforcement is also different. However, the ECR efficiency with cathodes on both sides of concrete
312 can be improved by prolonging the repair time and increasing the external potential.

313

314 **Author Contributions:**

315 **Xuandong Chen**: Conceptualization, Methodology, Writing- Original draft preparation, Software,
316 Investigation. **Qing Zhang:** Writing-reviewing and Editing, Methodology, conceptualization,
317 Supervision. **Feng Fu**: Data curation, Writing- Reviewing and Editing. **Yang Ming**: Software, Data
318 curation. **Hua Rong**: Methodology, Software, Conceptualization.

319

327 **Conflicts of Interest:** The authors declare no conflict of interest.

328

329 **References**

330 Arya, C., Vassie, P. and Bioubakhsh, S. (2014) 'Chloride penetration in concrete subject to wet–dry
331 cycling: influence of pore structure', *Proceedings of the Institution of Civil Engineers - Structures and*
332 *Buildings*, 167(6), pp. 343–354. doi: 10.1680/stbu.12.00067.

333 Bažant, Z. P. and Najjar, L. J. (1972) 'Nonlinear water diffusion in nonsaturated concrete', *Matériaux*

334   *et Constructions*, 5(1), pp. 3–20. doi: 10.1007/BF02479073.

335   Chen, X. *et al.* (2020) 'A multi-phase mesoscopic simulation model for the diffusion of chloride in

336   concrete under freeze–thaw cycles', *Construction and Building Materials*, 265, p. 120223. doi:

337   10.1016/j.conbuildmat.2020.120223.

338   Chen, X. *et al.* (2021) 'A multi-phase mesoscopic simulation model for the long-term chloride ingress

339   and electrochemical chloride extraction', *Construction and Building Materials*, 270, p. 121826. doi:

340   10.1016/j.conbuildmat.2020.121826.

341   DHIR, R. K., JONES, M. R. and MCCARTHY, M. J. (1993) 'PFA CONCRETE: CHLORIDE

342   INGRESS AND CORROSION IN CARBONATED COVER.', *Proceedings of the Institution of Civil*

343   *Engineers - Structures and Buildings*, 99(2), pp. 167–172. doi: 10.1680/istbu.1993.23375.

344   Du, X., Jin, L. and Ma, G. (2014) 'A meso-scale numerical method for the simulation of chloride

345   diffusivity in concrete', *Finite Elements in Analysis and Design*, 85, pp. 87–100. doi:

346   10.1016/j.finel.2014.03.002.

347   Fang, Y. *et al.* (2021) 'Investigation of electrochemical chloride removal from concrete using direct

348   and pulse current', *Construction and Building Materials*, 270, p. 121434. doi:

349   10.1016/j.conbuildmat.2020.121434.

350   Garcés, P., Sánchez De Rojas, M. J. and Climent, M. A. (2006) 'Effect of the reinforcement bar

351   arrangement on the efficiency of electrochemical chloride removal technique applied to reinforced

352   concrete structures', *Corrosion Science*, 48(3), pp. 531–545. doi: 10.1016/j.corsci.2005.02.010.

353   Jin, L. *et al.* (2015) 'Multi-scale analytical theory of the diffusivity of concrete subjected to mechanical

354   stress', *Construction and Building Materials*, 95, pp. 171–185. doi:

355   10.1016/j.conbuildmat.2015.07.123.

356   Kumar, S., Kumar, A. and Kujur, J. (2019) 'Influence of nanosilica on mechanical and durability

357   properties of concrete', *Proceedings of the Institution of Civil Engineers - Structures and Buildings*,

358   172(11), pp. 781–788. doi: 10.1680/jstbu.18.00080.

359   Li, L. Y. and Page, C. L. (1998) 'Modelling of electrochemical chloride extraction from concrete:

360   Influence of ionic activity coefficients', *Computational Materials Science*, 9(3–4), pp. 303–308. doi:

361   10.1016/s0927-0256(97)00152-3.

362   Li, L. Y. and Page, C. L. (2000) 'Finite element modelling of chloride removal from concrete by an

363   electrochemical method', *Corrosion Science*, 42(12), pp. 2145–2165. doi: 10.1016/S0010-

938X(00)00044-5.

Liu, Q. *et al.* (2015) 'A numerical study on chloride migration in cracked concrete using multi-component ionic transport models', *Computational Materials Science*, 99, pp. 396–416. doi: 10.1016/j.commatsci.2015.01.013.

Liu, Q. F. *et al.* (2014) 'Three-phase modelling of electrochemical chloride removal from corroded steel-reinforced concrete', *Construction and Building Materials*, 70, pp. 410–427. doi: 10.1016/j.conbuildmat.2014.08.003.

Liu, Q. feng *et al.* (2012) 'Multi-phase modelling of ionic transport in concrete when subjected to an externally applied electric field', *Engineering Structures*, 42, pp. 201–213. doi: 10.1016/j.engstruct.2012.04.021.

Mao, J. *et al.* (2015) 'Technology for Enhancing Durability of Structures of Sea-sand Concrete and Its Application', *Journal of Chinese Society for Corrosion and Protection*, 35, pp. 564–570.

Mao, J. *et al.* (2019) 'Hydrogen embrittlement risk control of prestressed tendons during electrochemical rehabilitation based on bidirectional electro-migration', *Construction and Building Materials*, 213, pp. 582–591. doi: 10.1016/j.conbuildmat.2019.04.008.

Martín-Pérez, B., Pantazopoulou, S. J. and Thomas, M. D. A. (2001) 'Numerical solution of mass transport equations in concrete structures', *Computers & Structures*, 79(13), pp. 1251–1264. doi: 10.1016/S0045-7949(01)00018-9.

Mazer, W., Lima, M. G. and Medeiros-Junior, R. A. (2018) 'Fuzzy logic for estimating chloride diffusion in concrete', *Proceedings of the Institution of Civil Engineers - Structures and Buildings*, 171(7), pp. 542–551. doi: 10.1680/jstbu.16.00153.

Miranda, J. M. *et al.* (2007) 'Limitations and advantages of electrochemical chloride removal in corroded reinforced concrete structures', *Cement and Concrete Research*, 37(4), pp. 596–603. doi: 10.1016/j.cemconres.2007.01.005.

Muthulingam, S. and Rao, B. N. (2014) 'Non-uniform time-to-corrosion initiation in steel reinforced concrete under chloride environment', *Corrosion Science*, 82, pp. 304–315. doi: 10.1016/j.corsci.2014.01.023.

Nguyen, T. H. Y. *et al.* (2021) 'Electrochemical chloride extraction on reinforced concrete contaminated external chloride: Efficiencies of intermittent applications and impacts on hydration products', *Cement and Concrete Composites*, 121, p. 104076. doi:

394   10.1016/j.cemconcomp.2021.104076.

395   Sánchez, M. and Alonso, M. C. (2011) 'Electrochemical chloride removal in reinforced concrete

396   structures: Improvement of effectiveness by simultaneous migration of calcium nitrite', *Construction*

397   *and Building Materials*, 25(2), pp. 873–878. doi: 10.1016/j.conbuildmat.2010.06.099.

398   Saraswathy, V., Lee, H.-S., *et al.* (2018) 'Extraction of chloride from chloride contaminated concrete

399   through electrochemical method using different anodes', *Construction and Building Materials*, 158, pp.

400   549–562. doi: 10.1016/j.conbuildmat.2017.10.052.

401   Saraswathy, V., Lee, H. S., *et al.* (2018) 'Extraction of chloride from chloride contaminated concrete

402   through electrochemical method using different anodes', *Construction and Building Materials*, 158, pp.

403   549–562. doi: 10.1016/j.conbuildmat.2017.10.052.

404   Shi, X. *et al.* (2012) 'Durability of steel reinforced concrete in chloride environments: An overview',

405   *Construction and Building Materials*, 30, pp. 125–138. doi: 10.1016/j.conbuildmat.2011.12.038.

406   Sun, G. *et al.* (2011) 'Multi-scale prediction of the effective chloride diffusion coefficient of concrete',

407   *Construction and Building Materials*, 25(10), pp. 3820–3831. doi: 10.1016/j.conbuildmat.2011.03.041.

408   Toumi, A., François, R. and Alvarado, O. (2007) 'Experimental and numerical study of

409   electrochemical chloride removal from brick and concrete specimens', *Cement and Concrete Research*,

410   37(1), pp. 54–62. doi: 10.1016/j.cemconres.2006.09.012.

411   Wang, Y., Gong, X. and Wu, L. (2019) 'Prediction model of chloride diffusion in concrete considering

412   the coupling effects of coarse aggregate and steel reinforcement exposed to marine tidal environment',

413   *Construction and Building Materials*, 216, pp. 40–57. doi: 10.1016/j.conbuildmat.2019.04.221.

414   Wang, Y., Li, L. Y. and Page, C. L. (2001) 'A two-dimensional model of electrochemical chloride

415   removal from concrete', *Computational Materials Science*, 20(2), pp. 196–212. doi: 10.1016/S0927-

416   0256(00)00177-4.

417   Wang, Yuanzhan *et al.* (2018) 'Prediction model of long-term chloride diffusion into plain concrete

418   considering the effect of the heterogeneity of materials exposed to marine tidal zone', *Construction and*

419   *Building Materials*, 159, pp. 297–315. doi: 10.1016/j.conbuildmat.2017.10.083.

420   Wu, L., Li, W. and Yu, X. (2017) 'Time-dependent chloride penetration in concrete in marine

421   environments', *Construction and Building Materials*, 152, pp. 406–413. doi:

422   10.1016/j.conbuildmat.2017.07.016.

423   Xia, J., Liu, Q., *et al.* (2018) 'Effect of environmental temperature on efficiency of electrochemical

424   chloride removal from concrete', *Construction and Building Materials*, 193, pp. 189–195. doi:

425   10.1016/j.conbuildmat.2018.10.187.

426   Xia, J., Liu, Q. feng, *et al.* (2018) 'Effect of environmental temperature on efficiency of

427   electrochemical chloride removal from concrete', *Construction and Building Materials*, 193, pp. 189–

428   195. doi: 10.1016/j.conbuildmat.2018.10.187.

429   Xia, J. *et al.* (2019) 'Numerical simulation of steel corrosion in chloride contaminated concrete',

430   *Construction and Building Materials*, 228, p. 116745. doi: 10.1016/j.conbuildmat.2019.116745.

431   Xia, J. *et al.* (2020) 'Effect of the stirrup on the transport of chloride ions during electrochemical

432   chloride removal in concrete structures', *Construction and Building Materials*, 250, p. 118898. doi:

433   10.1016/j.conbuildmat.2020.118898.

434   Xu, J. and Li, F. (2019a) 'Numerical analysis on efficiency of electrochemical chloride extraction of

435   one side anode in concrete', *Ocean Engineering*, 179(February 2017), pp. 38–50. doi:

436   10.1016/j.oceaneng.2019.03.018.

437   Xu, J. and Li, F. (2019b) 'Numerical analysis on efficiency of electrochemical chloride extraction of

438   one side anode in concrete', *Ocean Engineering*, 179, pp. 38–50. doi: 10.1016/j.oceaneng.2019.03.018.

439   Zhou, Y. *et al.* (2020) 'Reliability-based design analysis of FRP shear strengthened reinforced concrete

440   beams considering different FRP configurations', *Composite Structures*, 237, p. 111957. doi:

441   10.1016/j.compstruct.2020.111957.

442   Zhu, X. and Zi, G. (2017) 'A 2D mechano-chemical model for the simulation of reinforcement

443   corrosion and concrete damage', *Construction and Building Materials*, 137, pp. 330–344. doi:

444   10.1016/j.conbuildmat.2017.01.103.

445